



# Fractional anisotropy of the optic radiations correlates with the visual field after epilepsy surgery

João Paulo Sant Ana Santos de Souza<sup>1</sup> · Gabriel Ayub<sup>2</sup> · Pamela Castro Pereira<sup>1</sup> · José Paulo Cabral Vasconcellos<sup>2</sup> · Clarissa Yasuda<sup>1,3</sup> · Andrei Fernandes Joaquim<sup>3</sup> · Helder Tedeschi<sup>3</sup> · Brunno Machado Campos<sup>1</sup> · Fernando Cendes<sup>1,3</sup> · Enrico Ghizoni<sup>3</sup>

Received: 10 April 2019 / Accepted: 14 August 2019 / Published online: 7 September 2019

© Springer-Verlag GmbH Germany, part of Springer Nature 2019

## Abstract

**Purpose** This study assessed whether optic radiations (OR) microstructure after temporal lobe epilepsy (TLE) surgery correlated with visual field defects (VFD).

**Methods** Patients were subjected to diffusion tensor imaging (DTI) tractography of the OR and Humphrey perimetry after TLE surgery. We used Spearman's test to verify correlations between tractographic parameters and perimetry mean deviation. Tractographic variables were compared between patients with VFD or intact perimetry. Multiple logistic regression was applied between DTI and perimetry values. DTI sensitivity and specificity were assessed with a receiver operating characteristic (ROC) curve to evaluate VFD.

**Results** Thirty-nine patients had reliable perimetry and OR tractography. There was a significant correlation between (1) fractional anisotropy (FA) and both total ( $\rho = 0.569$ ,  $p = 0.0002$ ) and quadrant ( $\rho = 0.453$ ,  $p = 0.0037$ ) mean deviation and (2) radial diffusivity and total mean deviation ( $\rho = -0.350$ ,  $p = 0.0286$ ). There was no other significant correlation. Patients with VFD showed a significantly lower FA compared with patients with normal perimetry ( $p = 0.0055$ ), and a 0.01 reduction in FA was associated with a 44% increase in presenting VFD after surgery (confidence interval, CI = 1.10–1.88;  $p = 0.0082$ ). Using a FA of 0.457, DTI tractography showed a specificity of 95.2% and a sensitivity of 50% to detect VFD after surgery (area under the curve = 0.7619, CI = 0.6020–0.9218).

**Conclusion** The postoperative OR microstructure correlated with visual loss after epilepsy surgery. DTI postoperative OR tractography may be helpful in evaluating VFD.

**Keywords** Perimetry · Visual field defect · Optic radiations · Epilepsy surgery · Tractography

**Electronic supplementary material** The online version of this article (<https://doi.org/10.1007/s00234-019-02281-2>) contains supplementary material, which is available to authorized users.

✉ João Paulo Sant Ana Santos de Souza  
souza.medicine@gmail.com

<sup>1</sup> Neuroimaging Laboratory (LNI), University of Campinas (UNICAMP), Rua Vital Brazil, 251. Cidade Universitária Zeferino Vaz., Campinas, SP 13083-888, Brazil

<sup>2</sup> Department of Ophthalmology, University of Campinas (UNICAMP), Rua Tessália Vieira de Camargo, 126. Cidade Universitária Zeferino Vaz., Campinas, SP 13083-887, Brazil

<sup>3</sup> Department of Neurology and Neurosurgery, University of Campinas (UNICAMP), Rua Tessália Vieira de Camargo, 126. Cidade Universitária Zeferino Vaz., Campinas, SP 13083-887, Brazil

## Introduction

Temporal lobe epilepsy (TLE) is the most common variant of adult refractory epilepsies; one third of the cases will require surgical treatment for seizure control. Surgery is generally based on resection of the amygdala and hippocampus once hippocampal sclerosis (HS) is the main aetiology [1–3]. Even though surgery promotes a satisfactory seizure-free outcome and improves the quality of life, surgical resection may lead to visual field defects (VFD) [4, 5]. While approaching temporal mesial structures, the anterior portion of the temporal stem and lateral wall of the temporal horn can be injured. As a direct consequence, there can be damage to the optic radiations (OR) with associated quadrantanopia or even hemianopia [6–8].

Diffusion tensor imaging (DTI) is a non-invasive modality of white matter fibre evaluation that allows one to visualise tracts of interest three dimensionally using a voxel-based algorithm [9]. Besides a qualitative analysis, it allows one to determine the volume, number of streamlines and diffusivity metrics of the tracts [10]. Recent anatomical studies that involve DTI analysis documented Meyer's loop (ML) injury after epilepsy surgery, but no one assessed the relationship between OR microstructure tracked by DTI and the respective VFD observed postoperatively [6, 7, 11–16]. Generally, the distances between ML and the temporal pole (TP) are evaluated to guide safe temporal resections. There is concordance that white fibre loss leads to visual deficit, but whether this factor is the only and main one that explains VFD is poorly understood.

The main purpose of this study was to determine whether the OR microstructure status tracked by DTI correlated with postoperative VFD. Such evaluation may provide more accurate data on the real capacity of tractography to evaluate visual loss postoperatively. Our second aim was to assess a region-of-interest (ROI)-based strategy for the study of VFD after epilepsy surgery.

## Materials and methods

### Subjects and ethical aspects

This prospective cohort study involved patients with refractory TLE surgically treated in our teaching hospital. We included all patients from 2002 to 2017 with a diagnosis of mesial temporal lobe epilepsy (MTLE) with magnetic resonance imaging (MRI) evidence of HS observed at the outpatient clinic for refractory epilepsy who were subjected to either non-selective (modified anterior temporal lobectomy, mATL) or selective (transsylvian approach, TS) surgery [17–20]. Patients provided written informed consent, and project execution was approved by the ethical committee of our institution (CAAE 48049015.6.0000.5404).

Patients fulfilled the following criteria: older than 18 years of age, clinical semiology and electroencephalography (EEG) features compatible with MTLE, failure to achieve seizure control with at least two anti-epileptic drugs (appropriately chosen in terms of dosage, in isolated or combined regimens) [3, 21] and postoperative 3-T MRI (3T-MRI). We excluded patients with any additional confounding disease(s) (e.g. neoplasms and/or neurodegenerative disorders). All patients completed our institution's pre-surgical investigation protocol that includes at least video scalp-EEG monitoring and MRI [20]. We included only those patients who were positive for HS on MRI. Histopathology reports of all surgical samples were reviewed. All patients had HS according to the histopathological studies. Only one patient from the mATL group showed

additional focal cortical dysplasia in the temporal pole specimen (not identified in the preoperative MRI), besides HS.

### Postoperative DTI acquisition and processing

For tractography analysis, we acquired spin-echo single-shot echo planar imaging (EPI;  $2 \times 2 \times 2 \text{ mm}^3$  acquired voxel size, interpolated to  $1 \times 1 \times 2 \text{ mm}^3$ ; reconstructed matrix  $256 \times 256$ ; 70 slices; TE/TR 61/8500 msec; flip angle  $90^\circ$ ; 32 gradient directions; no averages; max b-factor =  $1000 \text{ s/mm}^2$ ; 6-min scan) and T1-weighted images (T1WI;  $1 \text{ mm}^3$  isotropic voxels, acquired in the sagittal plane; 1 mm thick; no gap; flip angle =  $8^\circ$ ; TR = 7.0 msec; TE = 3.2 msec; matrix =  $240 \times 240$ ; FOV =  $240 \times 240 \text{ mm}^2$ ). Image preprocessing and tensor calculation for all images was performed using the Explore DTI software (<http://www.exploredti.com>), A. Leemans, University Medical Center, Utrecht, The Netherlands). The images were corrected for temporal signal drift using diffusion weighted images (DWI), Gibbs ringing (to remove unwanted harmonics), movement and susceptibility artefacts by registering to the T1WI and were finally corrected for eddy currents. The fibre tractography was performed with a deterministic methodology based on a consistently reproduced ROI strategy that enables one to select the tract of interest. White matter tract changes were studied through fractional anisotropy (FA), mean diffusivity, axial diffusivity (AD), radial diffusivity (RD) and number of fibres (NF).

Tracking parameters were used as follows: (1) minimal FA for seed point selection = 0.2, (2) maximal FA for seed point selection = 1, (3) maximal angle =  $60^\circ$ , (4) step size = 1 mm, (5) minimal fibre length = 10 mm, (6) maximal fibre length = 500 mm and (7) seedpoint super sampling factor = [0 0 0].

### OR tractography

Two types of manually defined ROIs were used for tracking: "AND" and "NOT". The former is a restrictive ROI, which implies that streamlines out of this ROI will be deleted. The latter is an exclusion ROI: streamlines passing through this ROI will be deleted.

Herein, manually defined ROIs were allocated into two phases (Fig. 1). In other words, the gross track was derived from three ROIs: one NOT in the midline sagittal plane (to exclude interhemispheric fibres), one NOT in the axial plane surrounding the brainstem (at the level of the occipital lobe inferior border; to exclude corticospinal fibres), and one AND in the sagittal plane at the lateral boundary of the lateral geniculate body (to select fibres from the OR origin). The resulting tracked fibres allow identification of ML limits. Subsequently, the second phase required two ROIs: one NOT in the coronal plane anteriorly to the ML anterior aspect (to exclude neighbouring streamlines, such as the fornix) and

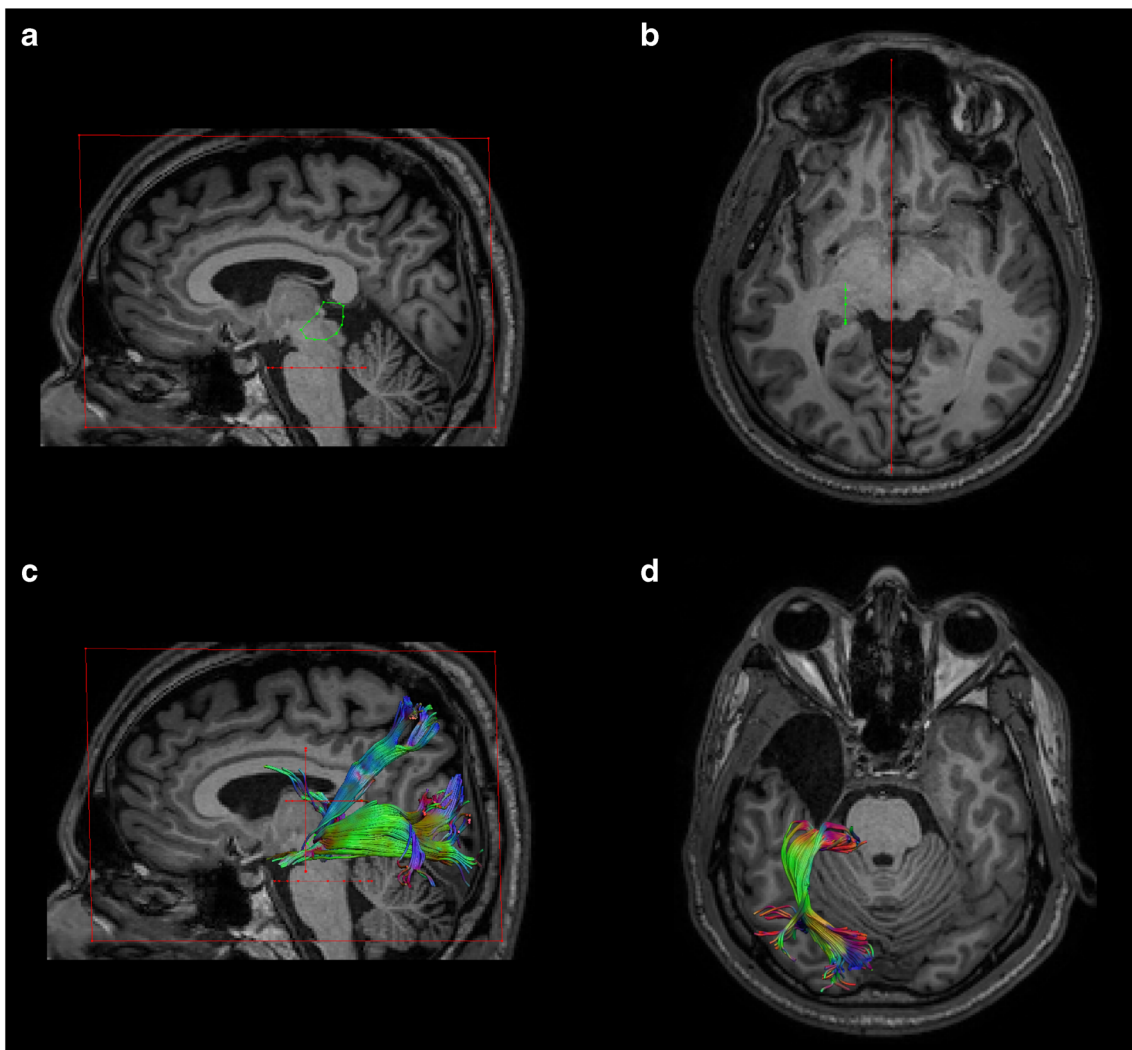


**Fig. 1** Tracking strategy of optic radiations fused with T1-weighted images. **a** Lateral view that shows two exclusion regions of interest (ROIs) in red and a restrictive ROI in green. Exclusion ROIs were placed in the midsagittal plane and around the brainstem. The restrictive ROI was allocated in the lateral portion of the lateral geniculate body (LGN). **b** Axial plane that shows the restrictive ROI from **a** in the lateral portion of the LGN as well as the exclusion ROI from **a** in the midsagittal plane. **c**

Lateral view demonstrates the tracts that result from the three ROIs shown in **a**. Two other exclusion ROIs (in red) were added: one in the axial plane above the LGN and another in the coronal plane anteriorly to Meyer's loop. **d** Superior view of the optic radiations resulting from the five aforementioned ROIs. Note, this patient was submitted to the modified anterior temporal lobectomy as suggested by the surgical lacunae in the left temporal lobe

one NOT in the axial plane (to exclude fibres that project to the parietal lobe).

### Perimetry

After surgery, patients were summoned by phone to perform standard 24-2 Humphrey digital perimetry. Prior to perimetry, all patients underwent best-corrected visual acuity in order to exclude comorbidities and refraction errors that could confer bias perimetry findings. Applied exclusion criteria were fixation loss  $\geq 20\%$ , false positive  $\geq 33\%$ , false negative  $\geq 33\%$ , perimetry performed in only one eye, previous ophthalmological comorbidity that could interfere with the result of

perimetry and the subject's refusal to participate in the study [22].

The technician who performed the exam was blinded to the surgical approach, outcome and the nature of this study. Once perimetry was concluded, the results were evaluated by a senior ophthalmologist who was aware of the temporal lobe surgery but was also blinded to the type of surgical approach.

Total and upper contralateral quadrant mean deviations were calculated for both eyes (ipsilateral and contralateral to surgery), based on perimetry findings. Mean deviation represents the degree of departure of the whole field's average values (from age-adjusted normal values). Perimetry findings were also classified categorically as incomplete or complete quadrantanopia or hemianopia [8, 23, 24].

## Statistical analysis

Due to the non-parametric distribution of our data, Spearman's correlation test was used to evaluate the correlation among FA, RD, mean diffusivity, AD and NF of the OR with both total and quadrant mean deviation. Patients were divided into two groups according to perimetry results: (1) those with VFD (incomplete or complete quadrantanopia or hemianopia) and (2) those with an intact visual field. DTI variables were compared between the two groups using the Mann-Whitney test. Associations between DTI and VFD were studied using multiple logistic regression with stepwise variable selection criteria. All DTI variables were considered for multiple regression analysis, and a stepwise  $p < 0.05$  was considered for entry into the model. DTI sensitivity and specificity to evaluate postoperative VFD were analysed with a receiver operating characteristic (ROC) curve. The significance level adopted in this study was 5%. Statistical analyses were performed with Statistical Analysis System for Windows version 9.4 software (SAS Institute Inc., Cary, NC, USA).

## Illustrative cases

Once patients underwent mATL and preoperative DTI acquisition, we could visually compare the pre- and postoperative OR. For illustrative purposes, we selected two cases in which the qualitative visual-based analysis was discordant to the perimetry results.

## Results

Ninety-three patients who underwent either TS amygdalohippocampectomy ( $n = 31$ ) or mATL ( $n = 62$ ) were enrolled in the study. From those, two refused to participate, eleven were lost at follow-up and two were excluded due to confounding ophthalmological comorbidities (one with bilateral keratoconus and one with glaucoma). From those patients who performed perimetry ( $n = 78$ ), thirty-five met our exclusion criteria, and four did not show identifiable streamlines compatible with OR in the postoperative tractography (although none of them showed hemianopia). From those without identifiable OR streamlines, three showed no loss(es) compatible with quadrantanopia or hemianopia, while one showed incomplete quadrantanopia. Demographic, tractographic and perimetric measures of patients who performed perimetry are presented in Tables 1 and 2.

The total mean deviation for both eyes (ipsilateral and contralateral to surgery) strongly correlated. The data indicated that our results reproduced the symmetrical loss pattern expected as a consequence of OR damage. The quadrant mean deviation also showed a strong correlation with the total mean deviation (Table 3).

**Table 1** Demography from patients who met all inclusion criteria ( $n = 39$ )

Characteristic	Value
Gender	
Male	18 (46.15%)
Side of surgery	
Left	23 (58.97%)
Age at surgery	40 ± 11.9 years
Time interval between	
Surgery and perimetry	5.53 ± 4.74 years
Surgery and DTI acquisition	4.78 ± 4.46 years
Surgical approach	
mATL	25 (64.1%)
Perimetric diagnosis	
mATL	
Incomplete quadrantanopia	5
Complete quadrantanopia	1
Incomplete hemianopia	2
Complete hemianopia	0
Transylvian approach	
Incomplete quadrantanopia	3
Complete quadrantanopia	4
Incomplete hemianopia	2
Complete hemianopia	1

Values represent the number of patients with the respective percentage. Means are followed by standard deviations

With regard to correlations, FA significantly correlated with total mean deviation from the ipsilateral ( $\rho = 0.56883$ ;  $p = 0.0002$ ) and contralateral ( $\rho = 0.52976$ ;  $p = 0.0005$ ) eyes. Correlation was also statistically significant between

**Table 2** Perimetric and tractographic measurements

Characteristic	Value
Perimetry	
Mean deviation	
Eye ipsilateral to surgery	
Total	− 4.04 ± 4.29 dB
Upper contralateral quadrant	− 8.13 ± 9.30 dB
Eye contralateral to surgery	
Total	− 3.07 ± 3.20 dB
Upper contralateral quadrant	− 7.67 ± 7.96 dB
Tractography of the OR	
Fractional anisotropy	0.479421178 ± 0.031350747
Radial diffusivity	0.000587422 ± 0.00005100
Mean diffusivity	0.000824121 ± 0.000052086
Axial diffusivity	0.001297521 ± 0.000071082
Fibres	221.08 ± 294.04

Values represent the mean followed by standard deviations

**Table 3** Spearman’s correlation between perimetric parameters

		Ipsilateral eye		Contralateral eye	
		Total mean deviation	Quadrant mean deviation	Total mean deviation	Quadrant mean deviation
Contralateral eye	Total mean deviation	rho = 0.840 <i>p</i> < 0.001	rho = 0.758 <i>p</i> < 0.001	NA	–
	Quadrant mean deviation	rho = 0.777 <i>p</i> < 0.001	rho = 0.809 <i>p</i> < 0.001	rho = 0.885 <i>p</i> < 0.001	NA
Ipsilateral eye	Total mean deviation	NA	–	–	–
	Quadrant mean deviation	rho = 0.920 <i>p</i> < 0.001	NA	–	–

Table shows the Spearman’s rho coefficient and the respective *p* value

FA and both ipsilateral (rho = 0.45358; *p* = 0.0037) and contralateral (rho = 0.46816; *p* = 0.0027) quadrant mean deviation. Radial diffusivity showed a significant negative correlation with total mean deviation from both eyes (rho = –0.35081, *p* = 0.0286 for the ipsilateral eye; rho = –0.31923, *p* = 0.0476 for the contralateral eye). No other tractographic variable was significantly correlated with perimetric parameters (Table 4). Scatterplots between perimetry and tractography are displayed in Fig. 2 and Online Resource 1.

Eighteen patients showed VFD, while twenty-one patients demonstrated no visual loss. The VFD group showed a significantly lower FA compared to the group with intact perimetry (*p* = 0.0055). Other tractographic variables did not differ between groups (Table 5 and Fig. 3). After the stepwise selection criteria, only the FA was selected among the variables (stepwise *p* = 0.0037). Our multiple regression analysis showed that an FA decrease of 0.01 was associated with a 44% increase of presenting VFD (*p* = 0.0082; odds ratio = 1.44, confidence interval, CI = 1.10–1.88).

Among DTI variables, FA showed the higher area under the ROC curve (AUC = 0.706, CI = 0.6020–0.9218; Table 6). An FA cut off of 0.457 to consider tractography positive or negative for VFD was associated with a specificity of 95.2% and a sensitivity of 50% (Fig. 4).

Patients who were submitted to mATL also underwent DTI acquisition prior to surgery. Figures 5 and 6 illustrate two cases in which the alterations in the macrostructure denoted

by the tractography do not explain the respective perimetry results.

## Discussion

### OR microstructure and macrostructure

DTI parameters may reflect fibre microstructure after surgery [25]. Surgical axonal transections should reduce FA and increase mean diffusivity. Indeed, Wallerian degeneration secondary to surgical white matter fibre transection comprises two phases: an acute one (days to weeks) characterised by fragmentation and dying-back of axons in which AD is reduced (representing axonal degeneration) and a second, chronic phase based on phagocytosis and myelin sheath loss (over weeks to months) that results in an RD increase (representing more water diffusion perpendicular to the long axis of the axon due to reduced myelin blockage in this direction) [26].

TLE surgery is not expected to directly damage the entire OR, but indirectly it may cause more global damage (homonymous hemianopia). The latter is secondary to the coagulation of small perimesencephalic vessels that arise from the anterior choroidal and posterior cerebral arteries [8, 27]. Thus, alterations that may represent other means of surgical damage are of great interest. Based on our results, we believe that FA is the

**Table 4** Spearman’s correlation between tractographic and perimetric parameters

		Fractional anisotropy	Radial diffusivity	Mean diffusivity	Axial diffusivity	Number of fibres
Eye Ipsilateral to surgery side	Total mean deviation	rho = 0.56883 <i>p</i> = 0.0002	rho = –0.35081 <i>p</i> = 0.0286	rho = –0.18381 <i>p</i> = 0.2627	rho = 0.08887 <i>p</i> = 0.5906	rho = 0.27908 <i>p</i> = 0.0853
	Quadrant mean deviation	rho = 0.45358 <i>p</i> = 0.0037	rho = –0.24997 <i>p</i> = 0.1248	rho = –0.11562 <i>p</i> = 0.4834	rho = 0.07037 <i>p</i> = 0.6704	rho = 0.25577 <i>p</i> = 0.1160
Eye Contralateral to surgery side	Total mean deviation	rho = 0.52976 <i>p</i> = 0.0005	rho = –0.31923 <i>p</i> = 0.0476	rho = –0.12267 <i>p</i> = 0.4569	rho = 0.16964 <i>p</i> = 0.3019	rho = 0.24436 <i>p</i> = 0.1338
	Quadrant mean deviation	rho = 0.46816 <i>p</i> = 0.0027	rho = –0.26703 <i>p</i> = 0.1003	rho = –0.11438 <i>p</i> = 0.4881	rho = 0.27485 <i>p</i> = 0.0904	rho = 0.27485 <i>p</i> = 0.0904

Table shows the Spearman’s rho coefficient and the respective *p* value

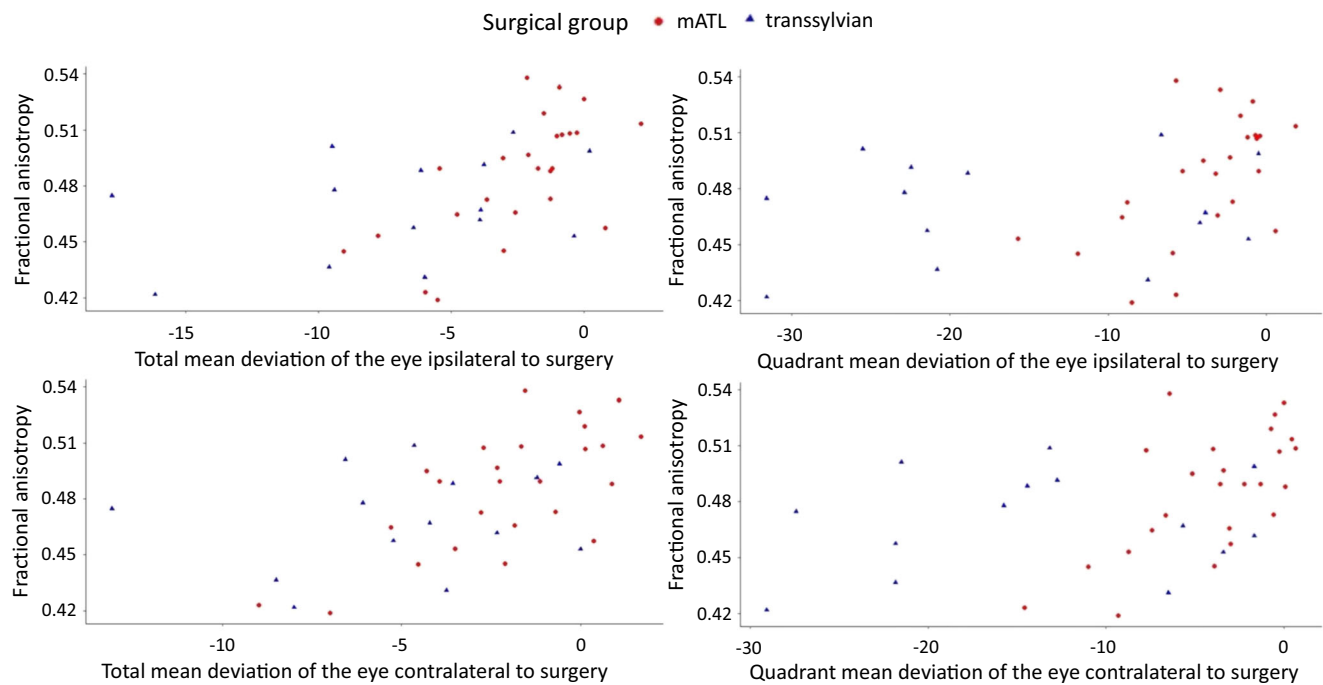


**Fig. 2** Scatterplots that show the distribution of DTI and perimetry variables according to the surgical approach. Red dots and blue triangles represent patients who underwent modified anterior temporal lobectomy (mATL) and the transylvian approach, respectively

principal and more durable microstructural parameter altered in the OR after surgery as well as the most appropriate to evaluate total and quadrant VFD.

Conversely with the aforementioned principles, our patients demonstrated OR microstructure alterations after epilepsy surgery. There was a significant correlation between FA and both total and quadrant mean deviation, results that suggest the more intense the visual defect, the lower the FA. It is also intriguing to recognise that FA in the central and posterior bundles are not distinctive enough from that observed in the more anterior streamlines. In other words, FA of regions less likely to be directly damaged appears to correlate with focal deficits caused by epilepsy surgery.

According to Fig. 2, patients who underwent TS (blue triangles) showed lower values of quadrant mean deviation compared to those patients who underwent mATL (red dots). Such a difference is based on the neuroanatomic relations between the OR and the landmarks used for each approach. The TS

requires an anteroposterior incision of 1–2 cm from the limen insulae through the inferior limiting sulcus in order to reach the lateral ventricle [18]. On the other hand, the mATL requires an anteroposterior incision at the rhinal sulcus to the limen insulae (posterior limit of the incision) to access the temporal horn [19]. Given the OR is located an average of 10.7 mm posterior to the limen insulae [28], injury to the Meyer's loop is more likely following the transylvian approach compared to the mATL.

In addition to FA, RD also significantly correlated with VFD. The mean postoperative DTI acquisition interval was 4.78 years, which explains why more earlier alterations, such as decreased AD, did not correlate with visual field loss. Correlation between RD and total mean deviation indicates that OR demyelination is likely to occur after epilepsy surgery and promote postoperative deficit.

We were unable to reconstruct any of the three OR bundles in four patients (~10% of our sample size with reliable

**Table 5** DTI comparison between groups with and without visual field defects

Variable	With VFD ( <i>n</i> = 18)	Without VFD ( <i>n</i> = 21)	<i>p</i> value
FA	0.46388 ± 0.03321	0.49274 ± 0.02294	0.0055
Mean diffusivity	0.00083 ± 0.00006	0.00082 ± 0.00005	0.9215
AD	0.00128 ± 0.00007	0.00131 ± 0.00007	0.2424
RD	0.00060 ± 0.00006	0.00058 ± 0.00004	0.2424
Streamlines	212.8889 ± 391.2730	228.0952 ± 190.4573	0.1507

Values represent the mean followed by standard deviations

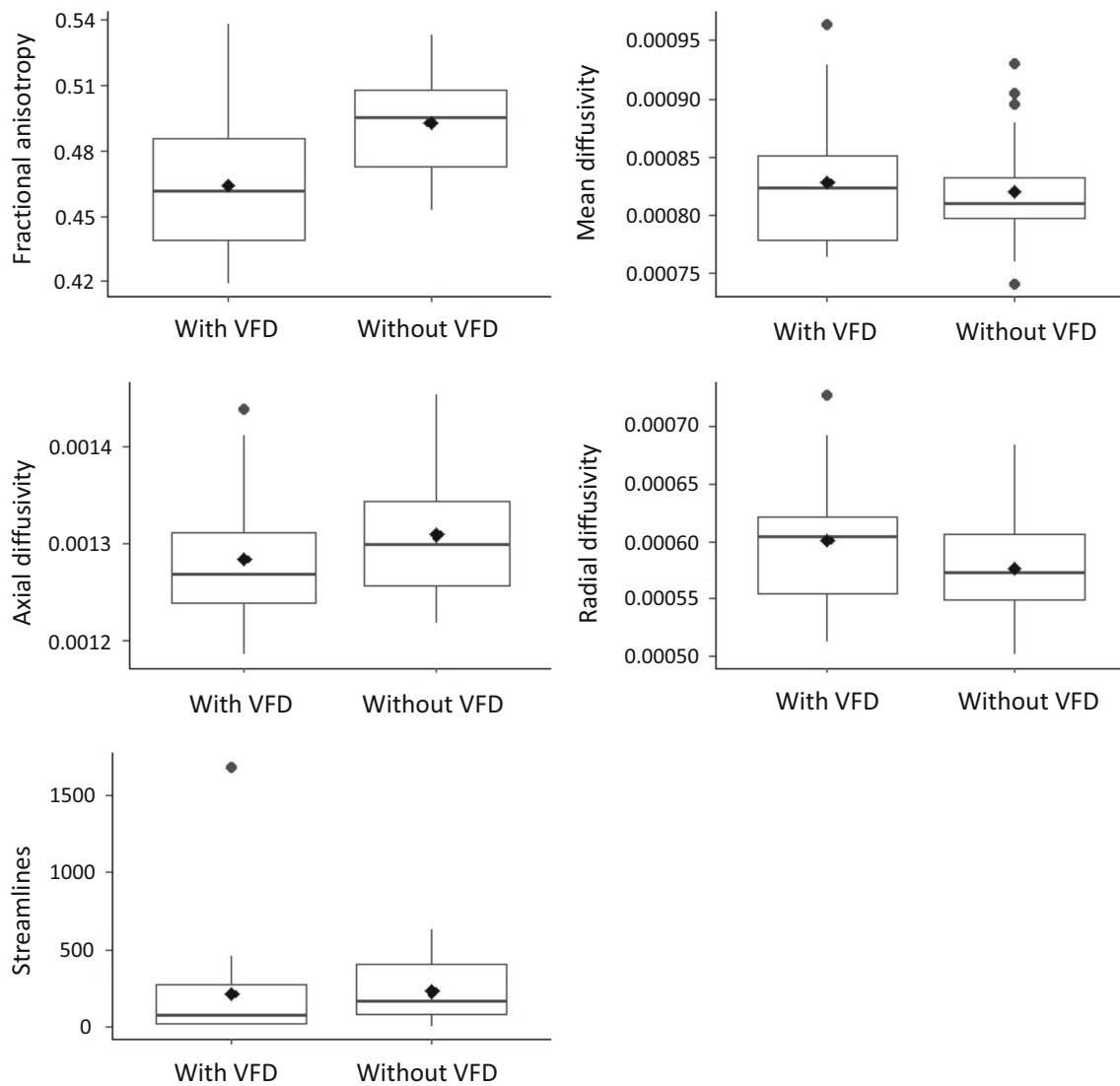


**Fig. 3** Boxplot that compares optic radiation tractography between groups with and without visual field defects (VFD). The lower and upper hinges correspond to the first and third quartiles (the 25th and 75th percentiles, respectively). The upper whisker extends from the hinge to the largest value no further than 1.5 times the interquartile range (IQR; distance between the first and third quartiles) from the

hinge. The lower whisker extends from the hinge to the smallest value at most 1.5 times the IQR of the hinge. Data beyond the end of the whiskers are called “outlying” points and are plotted individually as circular dots. The diamond dots represent the mean values. The horizontal line between the hinges corresponds to the median

**Table 6** ROC curve analysis of DTI to assess visual field defects

DTI variable	AUC	CI 95%	p value
Fractional anisotropy	0.7619	0.6020–0.9218	0.0021
Mean diffusivity	0.5106	0.3143–0.7069	0.4612
Axial diffusivity	0.6111	0.4285–0.7937	0.1171
Radial diffusivity	0.6111	0.4262–0.7960	0.1227
Streamlines	0.6362	0.4520–0.8205	0.0703

AUC, area under the curve; CI 95%, confidence interval of 95%; DTI, diffusion tensor imaging

perimetry). Intriguingly, two patients showed no visual loss, one patient had incomplete quadrantanopia and the other one showed visual loss not compatible with quadrantanopia/hemianopia. Thus, OR absence while attempting its tractography does not necessarily mean disruption due to surgical injury. Alternatively, technical problems during the MRI-DTI acquisition may justify the unsuccessful tracking. Another tractography limitation is the partial reconstruction of OR bundles. In a study involving six patients, Hofer et al. described the difficulty to fully reconstruct ML as well as the central and posterior bundles [29]. In our study, one patient (Fig. 6) appeared to present more streamlines in postoperative rather than preoperative DTI. Since streamline increases are

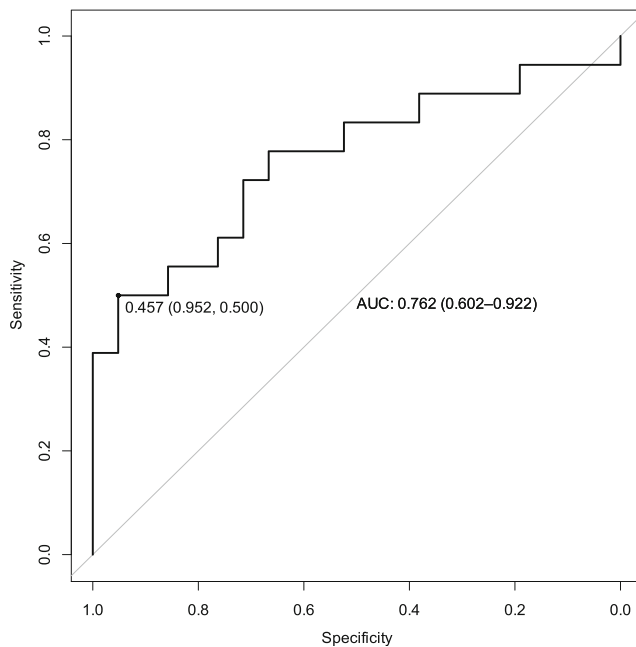


**Fig. 4** Receiver operating characteristic (ROC) curve of fractional anisotropy (FA) to assess visual field defects. An FA value of 0.457 showed a specificity of 95.2% and sensitivity of 50%. The FA area under the ROC curve (AUC) was 76.2%, with a 95% confidence interval of 0.602–0.955. This ROC curve showed  $p = 0.0021$

not expected after surgery—and the patient showed VFD—this case represents partial OR reconstruction in the preoperative acquisition. Analogously, another patient (Fig. 5) showed less streamlines after surgery. However, this phenomenon was not associated with VFD, a result that illustrates a case of partial postoperative OR reconstruction.

In the present study, the status of OR microstructure was superior to the OR macrostructure to evaluate visual field loss. In conjunction with current literature, we showed that loss of streamlines is not sufficient to solely explain postoperative VFD, and postoperative FA reduction of the OR is associated with increased VFD risk.

### Postoperative visual field evaluation

Automated perimetry is a satisfactory exam to evaluate the visual field due to its high reproducibility and low examiner influence. Our perimetric results confirmed that a considerable number of patients who underwent epilepsy surgery presented some degree of visual defects, a finding that reinforces the role of ophthalmological evaluation, mainly for those without co-registration of preoperative ML tractography and intraoperative MRI [30]. This indication is of relevance when we consider that post-surgery VFD precludes driving in 4–50% of seizure-free patients, and that patients are commonly unaware of the VFD [8, 31].

Some factors may interfere in visual field exam performance, and one of the most important is the learning effect.

This concept refers to improvement of visual field parameters as the patient becomes familiar with the visual field exam. In normal subjects, this effect increases the mean deviation on mid-periphery by 1–2 dB [32]. Due to this effect, some authors do not use the first perimetry exam in their evaluation, since they consider it imprecise [33–41].

A previous study found that education levels influence automated perimetry performance, especially for subjects with only elementary and secondary school education and illiterate people [42]. Another study revealed that the learning effect is present even in patients with high educational levels [43]. In our sample, a considerable number of patients (35 out of 78) were excluded due to non-reliable perimetry. Taking into account that the majority of our patients presented low education levels and cognitive impairment, DTI represents a complement to evaluate OR damage after epilepsy surgery.

Winston et al. demonstrated the utility of DTI in evaluating VFD after epilepsy surgery [14]. By using the co-registration between preoperative OR and structural postoperative MRI, they showed that all cases in which the resection margin surpassed the anterior aspect of the ML were associated with VFD. The extent of ML damage explained 65% of the VFD in the upper contralateral quadrant [14]. Indeed, the impaired fibre topography is also important to explain symptoms after epilepsy surgery. ML projects the contralateral upper field into the calcarine fissure, while the central and posterior bundles project the contralateral central and lower visual field, respectively [7]. Therefore, surgical damage restricted to more anterior OR portions leads to quadrantanopia, and an injury that extends to the posterior OR portions may cause hemianopia [44]. Given the significant correlation between FA and perimetry mean deviation, we believe that the OR microstructure complements the explanations about quadrant VFD as well as VFD in the entire contralateral hemifield. In this sense, OR fibres can be functionally impaired even if they are not transected by the surgical resection.

This study is an important contribution to the role of DTI in evaluating VFD after surgery. We not only showed the limitations of perimetry to evaluate postoperative patients (almost half of our patients did not achieve reliable perimetry), but we also developed an easy-to-use ROI-based strategy that significantly correlates with perimetry mean deviation and shows high specificity. For this reason, we suggest that a FA < 0.457 be considered evidence of VFD (quadrantanopia or hemianopia) for patients without reliable perimetry. When FA < 0.457, patients should be advised to avoid activities that require a satisfactory visual field (e.g. driving), even if they are seizure-free, until an accurate ophthalmological evaluation is performed.

### Limitations

The limitations of our study include the small sample size, absence of preoperative perimetry to compare with the



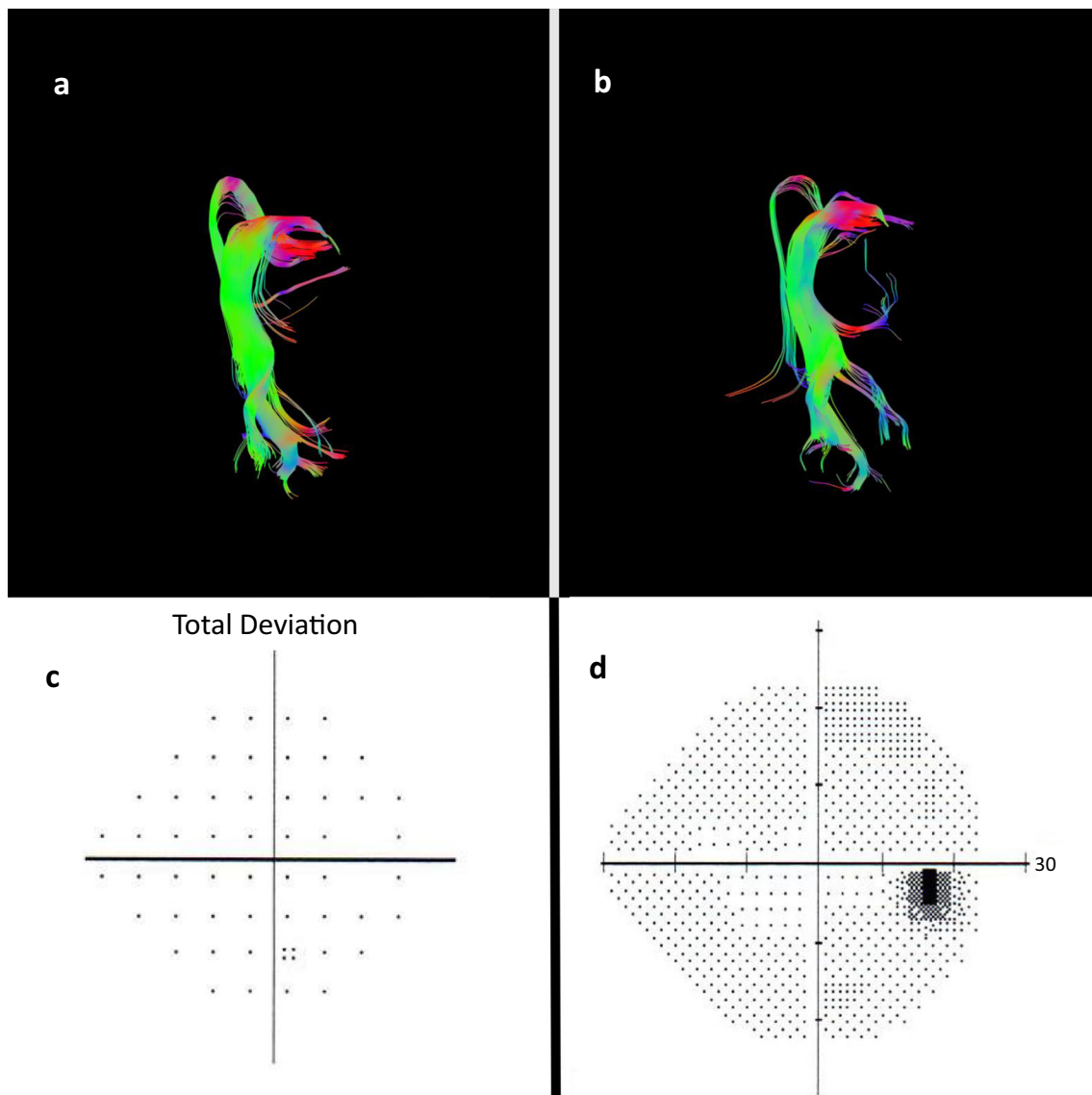


**Fig. 5** Illustrative case in which there is a putative decrease in the number of the optic radiation (OR) streamlines after surgery, but the respective perimetry demonstrates no visual field defect. **a** Superior view of the left OR preoperatively. **b** Superior view of the left OR from the same patient

postoperatively. **c** Postoperative perimetry shows the absence of black spots. **d** Postoperative perimetry shows normal qualitative results in the right eye of the same patient

postoperative measures (in order to detect new visual field defects caused by surgery), absence in standardising the postoperative time of perimetry acquisition and the fact that perimetry and DTI acquisition were not taken on the same day. These limitations indicate the difficulties to summon patients who usually have little-to-no financial resources (the majority of patients alleged no means of transport) and from a vast territory such as the one covered by our teaching hospital.

## Conclusion

Although surgical treatment is the gold standard for individuals with refractory TLE, it can lead to VFD. The rate of visual

complications is still high, and patients require common ophthalmological evaluations after epilepsy surgery, regardless of whether or not the approach is considered selective. Our results showed that postoperative FA and RD of the OR significantly correlated with total mean deviation after surgery. In the case of FA, there was also a significant correlation with visual field loss in the contralateral upper quadrant. Moreover, postoperative FA reduction was associated with an increased risk of VFD, data that evidence white fibres' reduction alone does not explain the visual field loss. This finding is corroborated by the fact that patients with VFD presented a significantly lower postoperative FA compared with patients with intact perimetry. Although DTI was not a sensitive method to screen VFDs (automated perimetry is still the gold

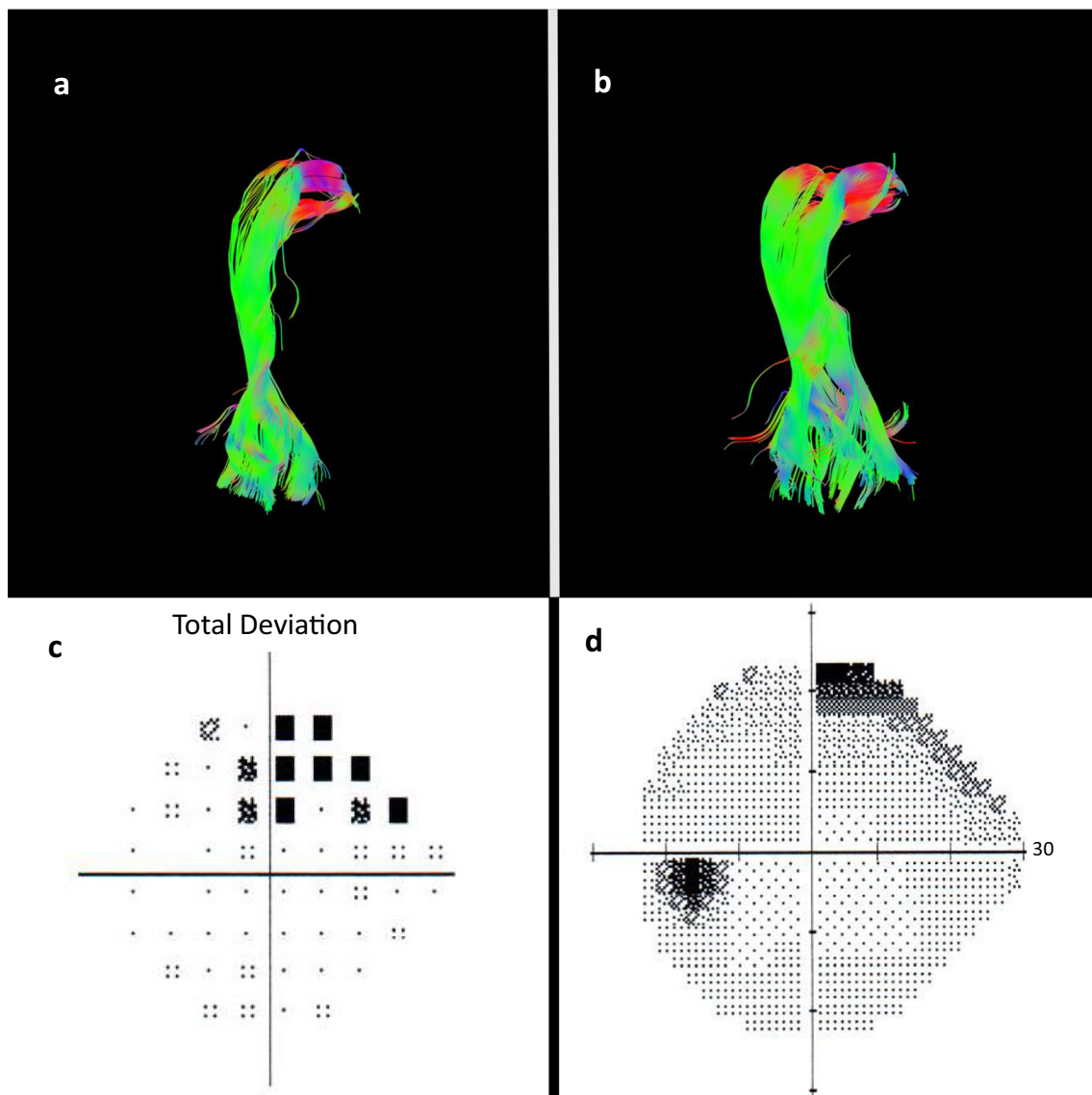


**Fig. 6** Illustrative case in which there is a putative increase in the number of the optic radiation (OR) streamlines after surgery, but the respective perimetry shows visual field defect. **a** Superior view of the left OR preoperatively. **b** Superior view of the left OR from the same patient

postoperatively. **c** Postoperative perimetry with black spots that incompletely occupy the contralateral upper quadrant. **d** Postoperative perimetry shows incomplete quadrantanopia in the left eye

standard), it is very specific. Further, FA findings suggestive of VFD can corroborate the automated perimetry findings while excluding the learning effect. This feature is very useful in a country like Brazil, which has very large physical dimensions, limited resources and low educational levels, to not repeat unnecessary exams.

**Funding information** This work was funded by the São Paulo Research Foundation (FAPESP).

### Compliance with ethical standards

**Conflict of interest** The authors declare that they have no conflict of interest.

**Ethical approval** All procedures performed in studies involving human participants were in accordance with the ethical standards of the institutional and/or national research committee and with the 1964 Helsinki declaration and its later amendments or comparable ethical standards.

**Informed consent** Informed consent was obtained from all individual participants included in the study.

### References

1. Wiebe S, Blume WT, Girvin JP, Eliasziw M (2001) A randomized, controlled trial of surgery for temporal-lobe epilepsy. *N Engl J Med* 345:311–318. <https://doi.org/10.1056/NEJM200108023450501>
2. Asadi-Pooya AA, Stewart GR, Abrams DJ, Sharan A (2017) Prevalence and incidence of drug-resistant mesial temporal lobe

- epilepsy in the United States. *World Neurosurg* 99:662–666. <https://doi.org/10.1016/j.wneu.2016.12.074>
3. Cendes F (2005) Mesial temporal lobe epilepsy syndrome: an updated overview. *J Epilepsy Clin Neurophysiol* 11:141–144. <https://doi.org/10.1590/S1676-26492005000300006>
  4. Tecoma ES, Laxer KD, Barbaro NM, Plant GT (1993) Frequency and characteristics of visual field deficits after surgery for mesial temporal sclerosis. *Neurology* 43:1235–1238
  5. Egan RA, Shults WT, So N, Burchiel K, Kellogg JX, Salinsky M (2000) Visual field deficits in conventional anterior temporal lobectomy versus amygdalohippocampectomy. *Neurology* 55:1818–1822
  6. Yogarajah M, Focke NK, Bonelli S, Cercignani M, Acheson J, Parker GJM, Alexander DC, McEvoy AW, Symms MR, Koeppe MJ, Duncan JS (2009) Defining Meyer's loop-temporal lobe resections, visual field deficits and diffusion tensor tractography. *Brain* 132:1656–1668. <https://doi.org/10.1093/brain/awp114>
  7. Dreessen de Gervai P, Sbotto-Frankensteen UN, Bolster RB, Thind S, Gruwel MLH, Smith SD, Tomanek B (2014) Tractography of Meyer's loop asymmetries. *Epilepsy Res* 108:872–882. <https://doi.org/10.1016/j.eplepsyres.2014.03.006>
  8. Yeni SN, Tanriover N, Uyanik Ö, Ulu MO, Özkara Ç, Karaağaç N, Ozyurt E, Uzan M (2008) Visual field defects in selective amygdalohippocampectomy for hippocampal sclerosis: the fate of Meyer's loop during the Transylvian approach to the temporal horn. *Neurosurgery* 63:507–515. <https://doi.org/10.1227/01.NEU.0000324895.19708.68>
  9. Winston GP, Mancini L, Stretton J, Ashmore J, Symms MR, Duncan JS, Yousry TA (2011) Diffusion tensor imaging tractography of the optic radiation for epilepsy surgical planning: a comparison of two methods. *Epilepsy Res* 97:124–132. <https://doi.org/10.1016/j.eplepsyres.2011.07.019>
  10. Winston GP (2012) The physical and biological basis of quantitative parameters derived from diffusion MRI. *Quant Imaging Med Surg* 2:254–265. <https://doi.org/10.3978/j.issn.2223-4292.2012.12.05>
  11. van Lanen RHGJ, Hoeberigs MC, Bauer NJC, Haeren RHL, Hoogland G, Colon A, Piersma C, Dings JTA, Schijns OEMG (2018) Visual field deficits after epilepsy surgery: a new quantitative scoring method. *Acta Neurochir* 160:1325–1336. <https://doi.org/10.1007/s00701-018-3525-9>
  12. Winston GP, Mancini L, Stretton J, Ashmore J, Symms MR, Duncan JS, Yousry TA (2011) Diffusion tensor imaging tractography of the optic radiation for epilepsy surgical planning: a comparison of two methods. *Epilepsy Res* 97:124–132. <https://doi.org/10.1016/j.eplepsyres.2011.07.019>
  13. Winston GP (2013) Epilepsy surgery, vision, and driving: what has surgery taught us and could modern imaging reduce the risk of visual deficits? *Epilepsia* 54:1877–1888. <https://doi.org/10.1111/epi.12372>
  14. Winston GP, Daga P, Stretton J, Modat M, Symms MR, McEvoy AW, Ourselin S, Duncan JS (2012) Optic radiation tractography and vision in anterior temporal lobe resection. *Ann Neurol* 71:334–341. <https://doi.org/10.1002/ana.22619>
  15. Lilja Y, Nilsson DT (2015) Strengths and limitations of tractography methods to identify the optic radiation for epilepsy surgery. *Quant Imaging Med Surg* 5:288–299. <https://doi.org/10.3978/j.issn.2223-4292.2015.01.08>
  16. Delev D, Wabbels B, Schramm J, Nelles M, Elger CE, von Lehe M, Clusmann H, Grote A (2016) Vision after trans-sylvian or temporobasal selective amygdalohippocampectomy: a prospective randomised trial. *Acta Neurochir* 158:1757–1765. <https://doi.org/10.1007/s00701-016-2860-y>
  17. Yaşargil MG, Wieser HG, Valavanis A, von Ammon K, Roth P (1993) Surgery and results of selective amygdala-hippocampectomy in one hundred patients with nonlesional limbic epilepsy. *Neurosurg Clin N Am* 4:243–261
  18. Yaşargil MG, Teddy PJ, Roth P (1985) Selective amygdalo-hippocampectomy. Operative anatomy and surgical technique. *Adv Tech Stand Neurosurg* 12:93–123
  19. Ghizoni E, Almeida J, Joaquim A, Yasuda C, de Campos B, Tedeschi H, Cendes F (2015) Modified anterior temporal lobectomy: anatomical landmarks and operative technique. *J Neurol Surg Part A Cent Eur Neurosurg* 76:407–414. <https://doi.org/10.1055/s-0035-1549303>
  20. Ghizoni E, Matias RN, Lieber S, de Campos BM, Yasuda CL, de Souza JPSAS, Pereira PC, Amato Filho ACS, Joaquim AF, Lopes TM, Tedeschi H, Cendes F (2017) Clinical and imaging evaluation of transuncus selective amygdalohippocampectomy. *World Neurosurg* 100:665–674. <https://doi.org/10.1016/j.wneu.2016.11.056>
  21. Kwan P, Schachter SC, Brodie MJ (2011) Drug-resistant epilepsy. *N Engl J Med* 365:919–926. <https://doi.org/10.1056/NEJMr1004418>
  22. Walsh TJ (2011) Visual fields: examination and interpretation. Oxford University Press, New York
  23. Hervás Navidad R, Altuzarra Corral A, Lucena Martín JA et al (2002) Defectos del campo visual en la cirugía resectiva de la epilepsia del lóbulo temporal. *Rev Neurol* 34:1025. <https://doi.org/10.33588/m.3411.2001505>
  24. Pathak-Ray V, Ray A, Walters R, Hatfield R (2002) Detection of visual field defects in patients after anterior temporal lobectomy for mesial temporal sclerosis-establishing eligibility to drive. *Eye (Lond)* 16:744–748. <https://doi.org/10.1038/sj.eye.6700152>
  25. Winston GP (2012) The physical and biological basis of quantitative parameters derived from diffusion MRI. *Quant Imaging Med Surg* 2:254–265. <https://doi.org/10.3978/j.issn.2223-4292.2012.12.05>
  26. Winston GP, Stretton J, Sidhu MK, Symms MR, Duncan JS (2014) Progressive white matter changes following anterior temporal lobe resection for epilepsy. *NeuroImage Clin* 4:190–200. <https://doi.org/10.1016/j.nicl.2013.12.004>
  27. Hughes TS, Abou-Khalil B, Lavin PJ et al (1999) Visual field defects after temporal lobe resection: a prospective quantitative analysis. *Neurology* 53:167–172
  28. Párraga RG, Ribas GC, Welling LC et al (2012) Microsurgical anatomy of the optic radiation and related fibers in 3-dimensional images. *Oper Neurosurg* 71:ons160–ons172. <https://doi.org/10.1227/NEU.0b013e3182556fde>
  29. Hofer S, Karaus A, Frahm J (2010) Reconstruction and dissection of the entire human visual pathway using diffusion tensor MRI. *Front Neuroanat* 4:15. <https://doi.org/10.3389/fnana.2010.00015>
  30. Winston GP, Daga P, White MJ, Micallef C, Misericocchi A, Mancini L, Modat M, Stretton J, Sidhu MK, Symms MR, Lythgoe DJ, Thornton J, Yousry TA, Ourselin S, Duncan JS, McEvoy AW (2014) Preventing visual field deficits from neurosurgery. *Neurology* 83:604–611. <https://doi.org/10.1212/WNL.0000000000000685>
  31. Winston GP (2013) Epilepsy surgery, vision, and driving: what has surgery taught us and could modern imaging reduce the risk of visual deficits? *Epilepsia* 54:1877–1888. <https://doi.org/10.1111/epi.12372>
  32. Heijl A (1989) The effect of perimetric experience in normal subjects. *Arch Ophthalmol* 107:81. <https://doi.org/10.1001/archoph.1989.01070010083032>
  33. Bengtsson B, Heijl A (1999) Inter-subject variability and normal limits of the SITA standard, SITA fast, and the Humphrey full threshold computerized perimetry strategies, SITA STATPAC. *Acta Ophthalmol Scand* 77:125–129
  34. Wild JM, Pacey IE, O'Neill EC, Cunliffe IA (1999) The SITA perimetric threshold algorithms in glaucoma. *Invest Ophthalmol Vis Sci* 40:1998–2009

35. Budenz DL, Rhee P, Feuer WJ et al (2002) Comparison of glaucomatous visual field defects using standard full threshold and Swedish interactive threshold algorithms. *Arch Ophthalmol* (Chicago, Ill 1960) 120:1136–1141
36. Budenz DL, Rhee P, Feuer WJ, McSoley J, Johnson CA, Anderson DR (2002) Sensitivity and specificity of the Swedish interactive threshold algorithm for glaucomatous visual field defects. *Ophthalmology* 109:1052–1058
37. Sekhar GC, Naduvilath TJ, Lakkai M et al (2000) Sensitivity of Swedish interactive threshold algorithm compared with standard full threshold algorithm in Humphrey visual field testing. *Ophthalmology* 107:1303–1308
38. Wild JM, Pacey IE, Hancock SA, Cunliffe IA (1999) Between-algorithm, between-individual differences in normal perimetric sensitivity: full threshold, FASTPAC, and SITA. Swedish Interactive Threshold algorithm. *Invest Ophthalmol Vis Sci* 40:1152–1161
39. Artes PH, Iwase A, Ohno Y, Kitazawa Y, Chauhan BC (2002) Properties of perimetric threshold estimates from full threshold, SITA standard, and SITA fast strategies. *Invest Ophthalmol Vis Sci* 43:2654–2659
40. Bengtsson B, Heijl A (1998) Evaluation of a new perimetric threshold strategy, SITA, in patients with manifest and suspect glaucoma. *Acta Ophthalmol Scand* 76:268–272
41. Shirato S, Inoue R, Fukushima K, Suzuki Y (1999) Clinical evaluation of SITA: a new family of perimetric testing strategies. *Graefes Arch Clin Exp Ophthalmol* 237:29–34
42. Aydin A, Kocak I, Aykan U, Can G, Sabahyildizi M, Ersanli D (2015) The influence of the learning effect on automated perimetry in a Turkish population. *J Fr Ophtalmol* 38:628–632. <https://doi.org/10.1016/j.jfo.2015.01.013>
43. Castro DPE, Kawase J, Melo LAS (2008) Learning effect of standard automated perimetry in healthy individuals. *Arq Bras Oftalmol* 71:523–528
44. Fraser JA, Newman NJ, Bioussé V (2011) Disorders of the optic tract, radiation, and occipital lobe. *Handb Clin Neurol* 102:205–221. <https://doi.org/10.1016/B978-0-444-52903-9.00014-5>

**Publisher's note** Springer Nature remains neutral with regard to jurisdictional claims in published maps and institutional affiliations.